

SUPPLEMENTARY INFORMATION

Anaerobic oxidation of methane alters sediment records of sulfur, iron and phosphorus in the Black Sea

Matthias Egger¹, Peter Kraal¹, Tom Jilbert^{1,2}, Fatimah Sulu-Gambari¹, Célia J. Sapart^{3,4}, Thomas Röckmann³ and Caroline P. Slomp¹

¹Department of Earth Sciences – Geochemistry, Faculty of Geosciences, Utrecht University, P.O. Box 80021, 3508 TA, Utrecht, The Netherlands

²Now at: Department of Environmental Sciences, Faculty of Biological and Environmental Sciences, University of Helsinki, P.O. Box 65 (Viikinkaari 2a), 00014 Helsinki, Finland

³Institute for Marine and Atmospheric Research Utrecht (IMAU), Utrecht University, Princetonplein 5, 3584 CC Utrecht, The Netherlands

⁴Laboratoire de Glaciologie, Université Libre de Bruxelles, Belgium

Correspondence to: Matthias Egger (m.j.egger@uu.nl)

1 Multicomponent model formulation

Molecular diffusion coefficients D_m (cm² yr⁻¹) were corrected for tortuosity in the porous medium according to Boudreau (1996).

$$D' = \frac{D_m}{1 - 2\ln(\phi)}$$

To account for sediment compaction, a depth-dependent porosity (ϕ) was described by

$$\phi(x) = \phi_\infty + (\phi_0 - \phi_\infty)e^{-\frac{x}{\gamma}}$$

where x is the distance from the sediment-water interface (cm), ϕ_∞ the porosity at depth in the sediment, ϕ_0 the porosity at the sediment surface, and γ the porosity attenuation factor (see Fig. S1 and Table S1).

The advective velocity of solids at depth v_∞ was described by

$$v_\infty = \frac{F_{sed}}{\rho(1 - \phi_\infty)}$$

where F_{sed} denotes the sediment accumulation rate (g cm⁻² yr⁻¹) and ρ the sediment density (1008 kg m⁻³) (Meysman et al., 2005).

24 **2 Supplementary tables**

25 **Table S1. Environmental parameters used by the diagenetic model.**

Parameter	Symbol	Value	Units
Porosity at surface	ϕ_0	0.97	-
Porosity at depth	ϕ_∞	0.61	-
Porosity e-folding distance	γ	95	cm
Sediment density	ρ	2.31	g cm^{-3}
Temperature	T	1	$^\circ\text{C}$
C:N ratio of organic matter	C/N	6.625	-
C:P ratio of organic matter	C/P	106	-
C:P ratio of organic matter under anoxia	C/P_{anoxic}	424	-
P:Fe ratio for $\text{Fe}(\text{OH})_3^{\text{a}}$	χ^{a}	0.1	-
P:Fe ratio for $\text{Fe}(\text{OH})_3^{\text{b}}$	χ^{b}	0.055	-
P:Fe ratio for $\text{Fe}(\text{OH})_3^{\text{c}}$	χ^{c}	0.03	-

26

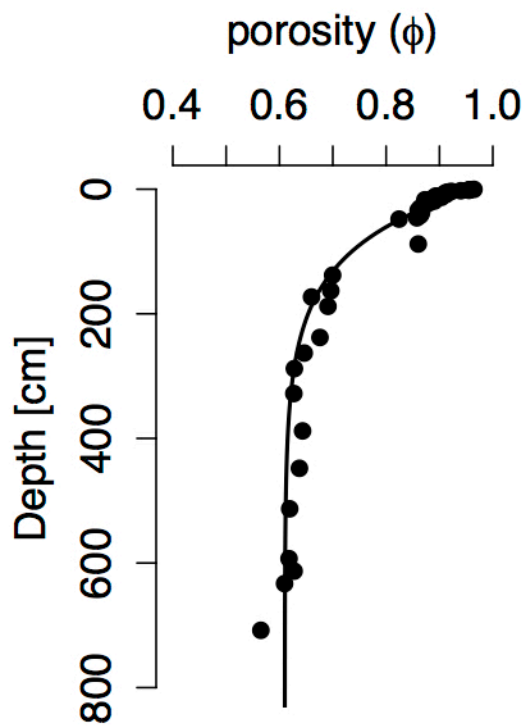
27 **Table S2. Time-dependent boundary conditions at the sediment surface.**

Parameter	> 9000 yrs B.P.	< 9000 yrs B.P.
J_{FeCO_3}	3.81	1.14
J_{S_0}	0	0
J_{CaP}	0.18	0.18
J_{DetrP}	0.32	0.095
$[\text{O}_2]$	0.18	0
$[\text{Fe}^{2+}]$	0	0
$[\Sigma\text{H}_2\text{S}]$	0	0.08
$[\text{CH}_4]$	0	0
$[\Sigma\text{NH}_4^+]$	0	0
$[\text{NO}_3^-]$	0	0
$[\text{H}_2\text{PO}_4^-]$	0	0
$[\text{DIC}]$	3	3

28 Fluxes have units of $\text{mmol m}^{-2} \text{yr}^{-1}$ and concentrations are in mmol L^{-1} . yrs B.P. = years before present.

29

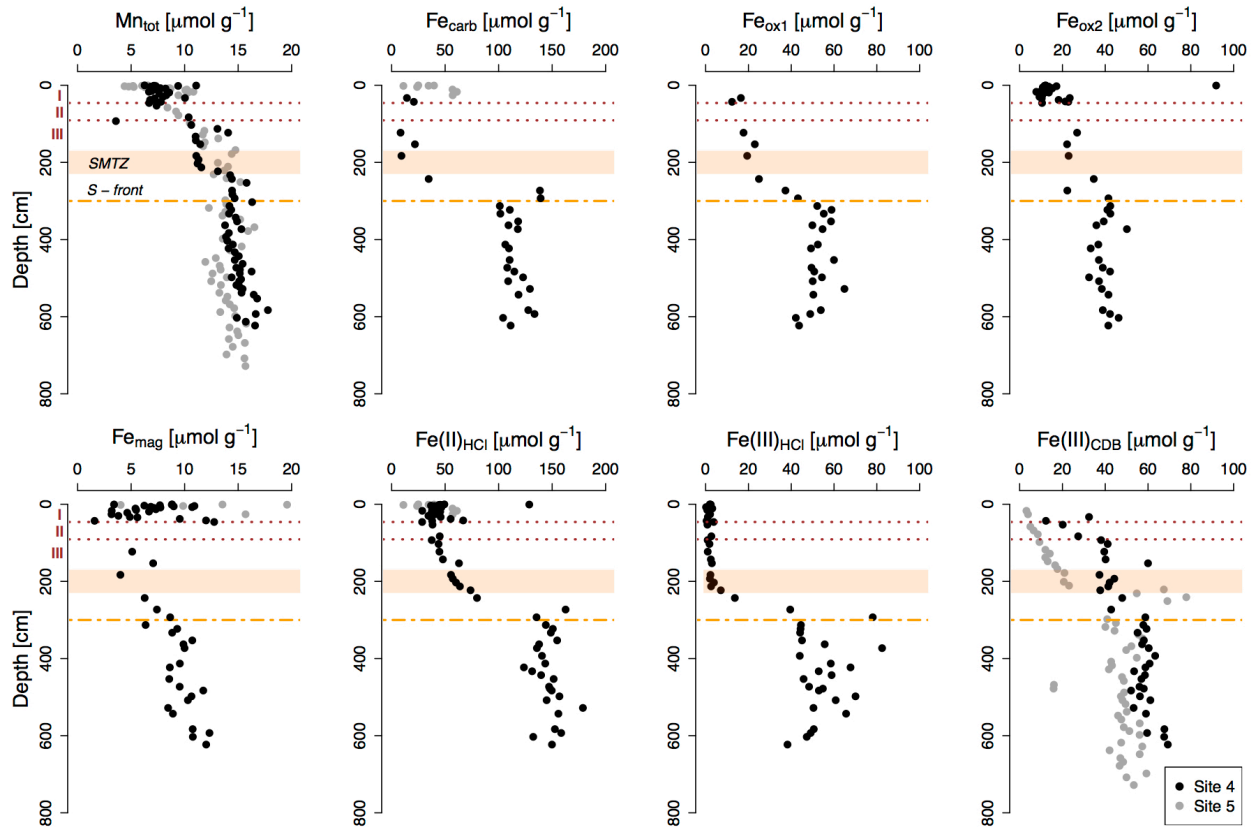
30



32

33 **Figure S1. Porosity measurements (black circles) and modeled porosity profile (black line) at site 4.**

34

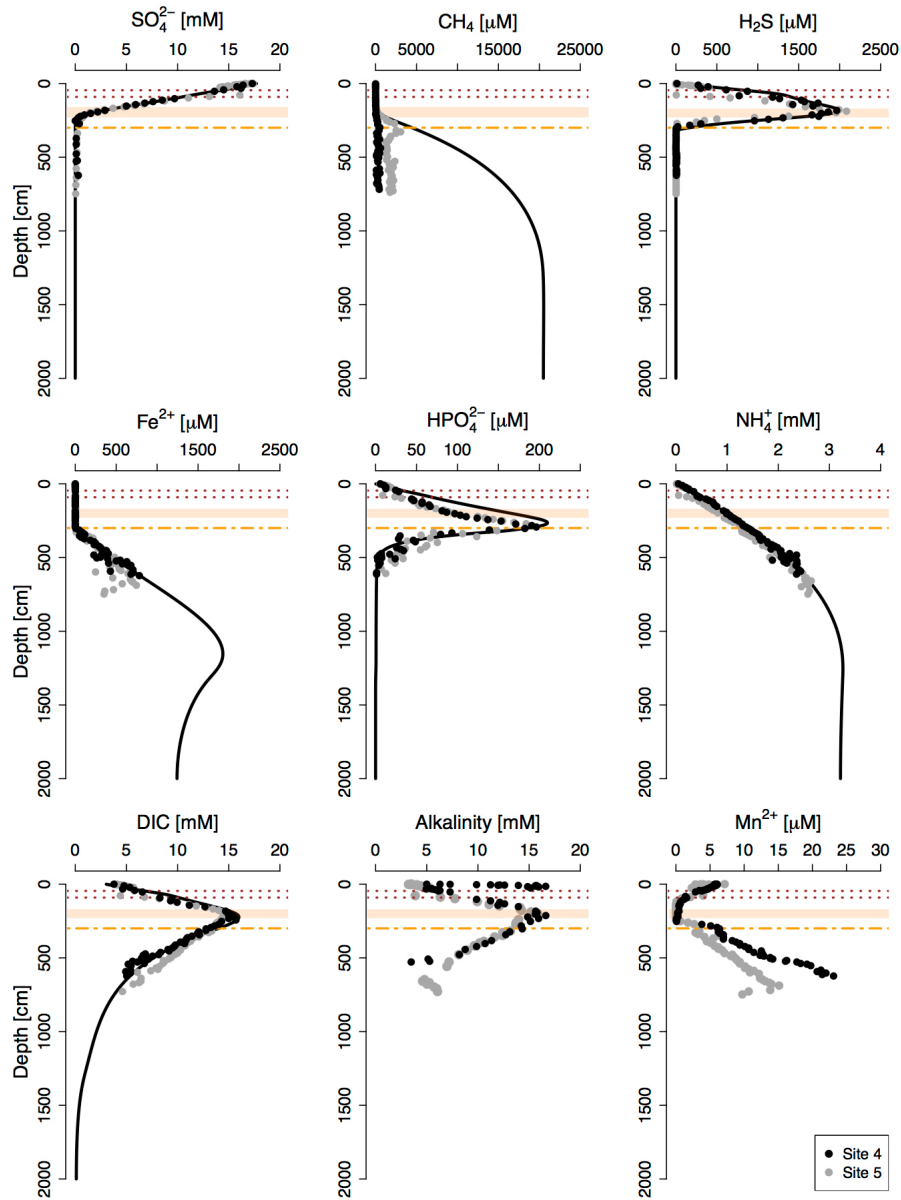


35

36 **Figure S2. Solid phase profile of total sedimentary Mn and Fe extraction results for site 4 (black dots) and 5 (grey dots).**
 37 **See Table 1 for a description of the different Fe phases. Note that Fe_{carb} is not corrected for dissolution of AVS during the**
 38 **Na acetate extraction step. $Fe(III)_{CDB}$ for site 5 represents the amount of Fe extracted during the CDB-step of the SEDEX**
 39 **P extraction. Red dotted lines and roman numbers indicate the transitions between the lithological Unit I (modern**
 40 **coccolith ooze), Unit II (marine sapropel) and Unit III (limnic deposits). The orange bar represents the sulfate-methane**
 41 **transition zone (SMTZ) and the orange dashed line shows the current position of the downward migrating sulfidization**
 42 **front (S-front).**

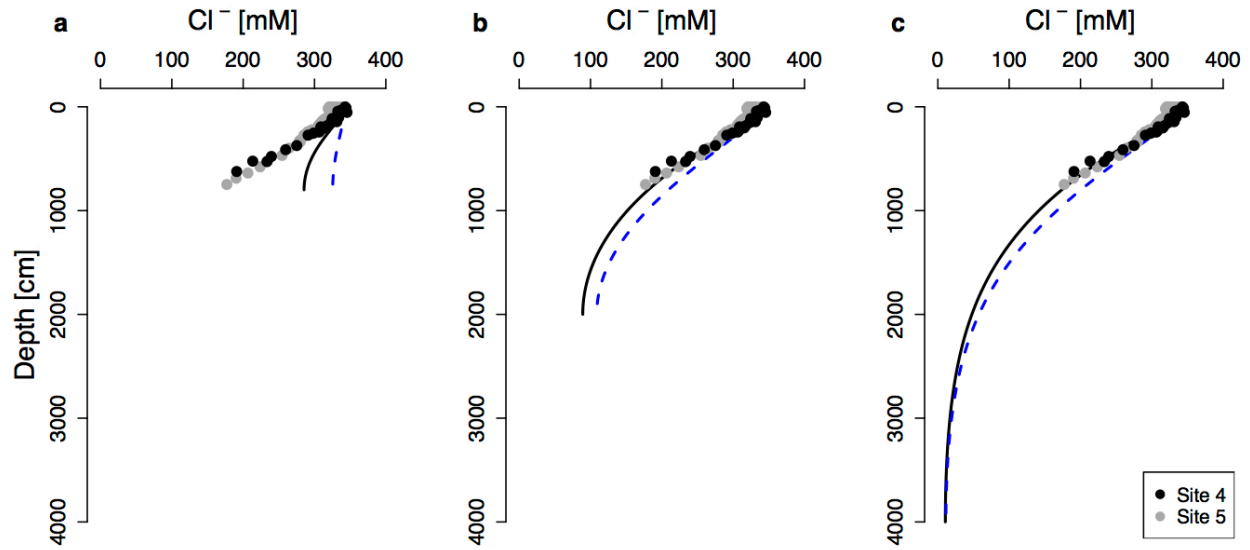
43

44



45

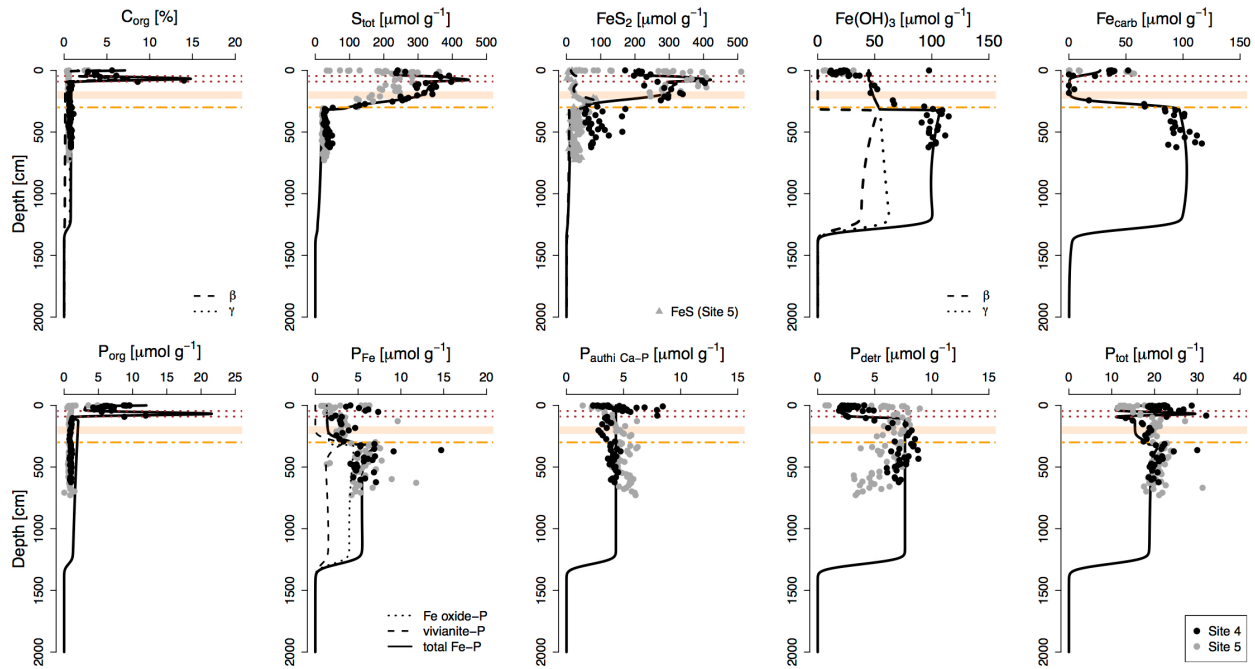
46 **Figure S3. Pore water profiles (whole model domain, i.e. 2000 cm) for site 4 (black dots) and 5 (grey dots). Black lines**
 47 **represent profiles derived from the diagenetic model. Red dotted lines and roman numbers indicate the transitions**
 48 **between the lithological Unit I (modern coccolith ooze), Unit II (marine sapropel) and Unit III (limnic deposits). The**
 49 **orange bar represents the sulfate-methane transition zone (SMTZ) and the orange dashed line shows the current position**
 50 **of the downward migrating sulfidation front.**



51

52 **Figure S4.** The influence of a zero gradient boundary condition at the base of the model domain on the pore water profile
 53 of chloride (Cl^-) is dependent on the modeled sediment depth. (a) Due to the transient diagenesis, a zero gradient is not
 54 reached within the depth range of the available data, i.e. the upper 800 cm. (b) A model length of 2000 cm results in a good
 55 fit of the modeled Cl^- profile with the measured pore water concentrations. Expanding the model domain to 4000 cm (c)
 56 largely increases the modeling time, with only minor improvement of the model fit. Thus, a depth range of 2000 cm was
 57 chosen in this study. The solid lines represent model simulations assuming an initial salinity of 1 for the freshwater phase
 58 and a linear increase to a salinity of 22 between 8500 and 100 years ago. Blue dashed lines, on the other hand, denote an
 59 increase in salinity from 1 to 22 between 8500 and 2000 years B.P., after which salinity stays constant, as proposed by
 60 Soulet et al. (2010).

61



63

64 **Figure S5.** Solid phase profiles (whole model domain, i.e. 2000 cm) for site 4 (black dots) and 5 (grey dots). Fe_{carb} was
 65 corrected for apparent AVS dissolution during the Na acetate extraction step (the uncorrected Fe_{carb} data is given in Fig.
 66 S2). Black lines represent profiles derived from the diagenetic model. Red dotted lines and roman numbers indicate the
 67 transitions between the lithological Unit I (modern coccolith ooze), Unit II (marine sapropel) and Unit III (limnic
 68 deposits). The orange bar represents the sulfate-methane transition zone (SMTZ) and the orange dashed line shows the
 69 current position of the downward migrating sulfidization front.

70

71 Supplementary references

72 Boudreau, B. P.: The diffusive tortuosity of fine-grained unlithified sediments, *Geochim. Cosmochim. Acta*, 60(16),
 73 3139–3142, 1996.

74 Meysman, F. J. R., Boudreau, B. P. and Middelburg, J. J.: Modeling reactive transport in sediments subject to
 75 bioturbation and compaction, *Geochim. Cosmochim. Acta*, 69(14), 3601–3617, 2005.

76 Soulet, G., Delaygue, G., Vallet-Coulomb, C., Böttcher, M. E., Sonzogni, C., Lericolais, G. and Bard, E.: Glacial
 77 hydrologic conditions in the Black Sea reconstructed using geochemical pore water profiles, *Earth Planet. Sci. Lett.*,
 78 296(1-2), 57–66, 2010.

79